2024, 21(3): 1101-1118
https://dx.doi.org/10.21123/bsj.2023.8340
P-ISSN: 2078-8665 - E-ISSN: 2411-7986
Baghdad Science Journal

Deep Learning Techniques in the Cancer-Related Medical Domain: A Transfer Deep Learning Ensemble Model for Lung Cancer Prediction

Omar Abdullatif Jassim* [*1], Mohammed Jawad Abed [1], Zenah Hadi Saied [2]

[1]Department of Medical Instrumentation Techniques Engineering, Al Hikma University College, Baghdad, Iraq.
[2]Department of Medical Laboratory Technologies, Institute of Medical Technology-Al-Mansour, Middle Technical University, Baghdad, Iraq.
*Corresponding Author.

Received 08/01/2023, Revised 01/04/2023, Accepted 02/04/2023, Published Online First 20/08/2023, Published 01/03/2024

Abstract

Problem: Cancer is regarded as one of the world's deadliest diseases. Machine learning and its new branch (deep learning) algorithms can facilitate the way of dealing with cancer, especially in the field of cancer prevention and detection. Traditional ways of analyzing cancer data have their limits, and cancer data is growing quickly. This makes it possible for deep learning to move forward with its powerful abilities to analyze and process cancer data. Aims: In the current study, a deep-learning medical support system for the prediction of lung cancer is presented. Methods: The study uses three different deep learning models (EfficientNetB3, ResNet50 and ResNet101) with the transfer learning concept. The three models are trained using a CT lung cancer dataset consisting of 1000 images and four different classes. The data augmentation process is applied to prevent overfitting, increase the size of the data, and enhance the training process. Score-level fusion and ensemble learning are also used to get the best performance and solve the low accuracy problem. All models were evaluated using accuracy, precision, recall, and the F1-score. Results: Experiments show the high performance of the ensemble model with 99.44% accuracy, which is better than all of the current state-of-the art methodologies. Conclusion: The current study's findings demonstrate the high accuracy and robustness of the proposed ensemble transfer deep learning using various transfer learning models.

Keywords: Breast cancer, Cancer prediction, Deep learning, Ensemble learning, Lung cancer, Machine learning, Medical engineering.

Introduction

Countless cells make up human bodies. When one of these cells starts growing in an uncontrolled and unnatural way due to cellular alterations, cancer invades this cell [1].

According to World Health Organization (WHO) statistics, cancer is the second leading cause of death [2,3].

Hundreds of thousands of cancer cases are registered every year. For men and women, respectively, the probability of dying from cancer is 7.34% and 6.28%. Lung and oral cavity cancers were defined as the causes of 25% of cancer deaths in men, and breast and oral cavity cancers were the causes of 25% of cancer deaths in women [1].

2024, 21(3): 1101-1118
https://dx.doi.org/10.21123/bsj.2023.8340
P-ISSN: 2078-8665 - E-ISSN: 2411-7986
Baghdad Science Journal

Cancer statistics change every year. According to 2018 [4], 2019 [5], 2020 [6], 2021 [7] and 2022 [8] statistics, the most common causes of cancer are illustrated as percentages in Table 1.

Table 1. Cancer statistics (A) Indian 2018 statistics (B) Global 2018 statistics (C) Global 2020 Statistics.

Network	*Breast*	*Lung*	*Prostate*	*Stomach*	*Thyroid*	*Cervix Uetri*	*colorectum*	*Leukaemia*	*Others*
2018	19.9%	12.5%	-	-	8.6%	7.8%	5.7%	5.2%	40.3%
2019	15.24%	12.94%	9.9%	-	2.14%	3.51%	8.3%	3.5%	44.47%
2020	11.72%	11.4%	7.3%	5.6%	3%	3.1%	10%	-	47.7%
2021	14.83%	12.42%	13.09%	-	3%	3.5%	7.87%	3.21%	42.08%
2022	15%	12.34%	13.99%	-	1.66%	3.43%	7.87%	3.16%	42.55%

According to [9], lung cancer was the deadliest cancer in 2020. Liver, stomach, and breast cancer were also the next three deadliest cancers, with percentages of 8.3%, 7.7% and 6.9%, respectively. Fig 1, shows the global cancer-death statistics through 2020 [9,10].

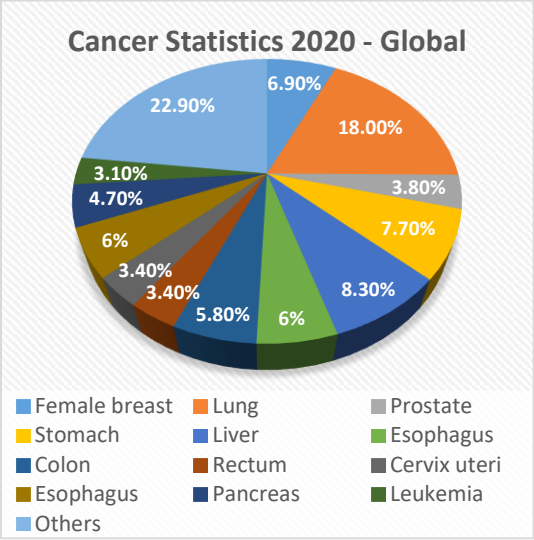

Figure 1. Cancer statistics

The Cancer Facts and Figures report estimated the number of cancer cases in 2022 at 1918030 cases. The report indicated that the deadliest men-related cancer from 1930 to 2019 was lung cancer. The top three cancers are stomach, colon, and prostate cancer. On the other hand, for women, the cancer percentages were lower than for men. However, lung cancer also recorded the most death cases among women. The next three most common cancers for women were breast, stomach and colon [11].

The main contribution of the current study can be summarized as follows:

- Solve the problem of the low accuracy of lung cancer prediction systems by proposing ensemble and fusion techniques.
- Introduce a new medical support tool for lung cancer prediction.
- Take into account the main lung cancer classes and classify them accordingly.
- Use small and efficient deep-learning models.

The rest of the paper will be organized as follows: First, the related work will be listed and compared. Then, the proposed materials and

2024, 21(3): 1101-1118
https://dx.doi.org/10.21123/bsj.2023.8340
P-ISSN: 2078-8665 - E-ISSN: 2411-7986
Baghdad Science Journal

methods will be introduced and illustrated. After that, the results will be included and a detailed discussion will be introduced. The limitations of the paper and the conclusion will be listed at the end of the paper. The recommendation and future work will also be included in the conclusion section.

Related Work

Because of the huge amount of multimodality data that has come in over the past ten years, the use of data analysis in health information systems has grown a lot.

In the field of medical health, the interest in developing machine learning (ML) models to manipulate and process this huge amount of medical data has increased significantly [12].

In recent years, Deep Learning (DL), a method built on artificial neural networks, has emerged as a high-performance machine learning methodology that holds the potential to transform the field of artificial intelligence [12].

Using DL in medical fields is very effective and has recorded many achievements that were previously hard to handle. DL presents different types of networks with many capabilities that can handle a huge amount of medical data (textual information, audio signals, medical images, and videos). These DL networks (models) provide a very powerful tool for many medical platforms [13-15].

Cancer prevention[16-18], cancer detection[19-21], COVID-19 detection[22-24], medical information analysis[25-27], and many other medical fields have used the efficiency of ML and DL models.

Many DL models are used in the medical domain. The nature of the medical field, the size of processed information, and the aim of research define the type and architecture of the DL network. Table 2 lists the most commonly used DL networks in the medical domain and their properties.

Table 2. Common DL networks in the medical domain.

Network	Architecture characteristics	Description	Remarks
Deep auto encoder[28]	D=2 or more. Input and output layers have the same number of neurons.	Used in unsupervised learning. Used in dimension transformation or reduction. Used for feature extraction and selection.	Requires a pre-training stage. Suffers from the gradient vanishing problem.
Deep Boltzmann Machine [29]	Undirected layers. D=2 or more. The layers are either visible or hidden and there are no input/output layers.	The undirected connections allow supervised and unsupervised learning.	Consumes too much time for learning. Not suitable for large datasets.
Convolutional Neural Networks[30]	Consists of: Convolution, pooling, fully-connected and classification layers. Uses non-linear activation function. Accepts its input as image directly.	Used in medical image classification problems (cancer detection, COVID19 detection, disease detection)	Apply the feature extraction step inside the network. Not all neurons are connected. Needs too much data to learn.
ResNet50 [31]	Advanced type of CNN 50-layer deep Consists of residual units (skipping connections)	Used in medical image classification with better performance	Needs training time more than CNN, but its performance is much better. Needs too much data to learn.
GoogleNet [32]	Another type of CNN The main concept is the inception layers (works in parallel) with different kernel size.	Used in medical image classification with good performance	Needs training time less than ResNet50, but its performance is not better than ResNet50. Needs too much data to learn.
EfficientNet [33]	Convolutional neural networks supported by scaling method (scale dimension of	Used in many image classification problems.	It is smaller and faster than ResNet. It reduces battery usage. It is efficient for deep learning

2024, 21(3): 1101-1118
https://dx.doi.org/10.21123/bsj.2023.8340
P-ISSN: 2078-8665 - E-ISSN: 2411-7986
Baghdad Science Journal

depth/width/resolution). mobile applications.

Hundreds of studies are introduced in the medical domain every year. Many of these researches use the ML and DL capabilities[34]. Table 3 includes the most recent studies that use deep learning models in the cancer prevention and detection fields.

Table 3. A comparative study of the most recent deep learning models in the cancer prevention and detection fields

Study	Field description	DL model	Dataset	Results
Khan et al. [35]	Breast cancer detection and classification	CNN, GoogleNet, VGG, ResNet	8000 images	ACC: 97.5%
Selvathi & Aarthy [36]	Breast cancer detection	CNN, Sparse Auto-Encoder (SAE)	Mammograms (mini-MIAS)	ACC: 97%
Zhang et al [37]	Breast Cancer detection and classification	ResNet50	CLEF-15: 6776 CLEF-16: 10942 ISIC-16: 1279 SIC-17: 2750	ACC=76.6% ACC=87.3% ACC=85.5% ACC=90.2%
Haşim [21]	Breast Cancer Detection	DCNN	MRI images including 198 malignant and 102 benign cases.	ACC=98.33%
Mukhlif et al. [38]	Breast Cancer classification	XceptionNet	ICIAR 2018 dataset	ACC= 99%
Mahbod et al. [39]	Skin cancer prediction	AlexNet, VGG16 and ResNet-18	150 validation images of the ISIC challenge	AUC= 83.83% for melanoma. AUC= 97.55% for seborrheic keratosis
Samala et al. [40]	Breast Cancer detection	Multi-stage transfer learning	DBT: 1797 malignant and 2242 benign	AUC=0.91
Li et al. [41]	Breast Cancer mass classification	Pretrained VGG16 network	441 patients with both DBT and FFDM	$\Delta AUC = 0.010 \pm 0.008$, $p < 0.001$; $\Delta AUC = 0.009 \pm 0.005$, $p < 0.001$
Nagpal et al. [42]	Prostate cancer detection	CNN+Gleason pattern	331 slides of TCGA	ACC=70%
Alakwaa et al. [19]	Lung cancer detection	3DCNN	Images of 1397 patients of DSB dataset and 888 patients of LUNA16 dataset	ACC=86.6%
Ardila et al. [43]	Lung cancer screening	3D CNN	6,716 National Lung Cancer Screening Trial cases	AUC= 0.94
Benhammou et al. [20]	Breast cancer detection	CNN	7909 cases of BreakHis dataset	ACC=88.9%
Xie et al. [44]	Pulmonary nodule detection	R-CNN, 2D CNN	LUNA-16	ACC=86.4%
Coudray et al. [45]	Non-small Lung cancer detection	Inception V3	1634 lung images	ACC=85.6%
Ahmed Ech-Cherif et al. [46]	Skin Cancer Detection	mobile-ready deep neural network	DermNet, ISICy Archive, and Dermofit Image Library	ACC= 91.33%
Guo et al. [47]	Cervix and non-cervix detection	Customized CNN, inception method	Training: MobileODT, Kaggle, COCO2017, Test: SEVIAaa	ACC= 91.6 F1-score =89%

2024, 21(3): 1101-1118
https://dx.doi.org/10.21123/bsj.2023.8340
P-ISSN: 2078-8665 - E-ISSN: 2411-7986
Baghdad Science Journal

Hu et al. [48]	Cervical pre-cancer detection	RetinaNet,	Microsoft COCO images, 7334 training images, 970 validation images, and 1058 test images	AUC=0.95
Senthilkumar et al. [49]	Cervical Cancer	Ensemble Learning	300 samples taken from GSE44001	ACC= 92.69%
Alzubaidi et al.[50]	Transfer Learning Medical Imaging	DCNN	200,000 unlabeled images of skin cancer	F1-score= 98.53%
Ashokkumar [51]	Axillary lymph node breast cancer prediction	Kohonen self-organizing ANN	1050 images of 850 individual	ACC=94%
Lang et al. [52]	Oropharyngeal Cancer prediction	3D CNN	412 patient cases of OPC dataset, 263 cases of HNSCC dataset for training. 90 cases of HN PET-CT for validation. 80 cases of HN1 for test.	AUC= 0.81
Me et al. [53]	Breast cancer pathology	Two stage of deep and machine learning	486 cases of H&E-stained pathology	ACC (Val) =88.15% ACC(test)=90.43%
Hu et al. [54]	Gastric cancer detection	CNN	245,196 cases	ACC=96.47%
Zhao et al. [55]	Gastric cancer detection	AlexNet, ResNet, VGG, Inception, DenseNet, Deeplab	99,777 individuals, 1,422,523 images	ACCs are between 77.3 and 98.7%
Tung et al. [56]	Pathological slices gastric cancer detection	CNN YOLOv4	13,600 of 50 individuals	Sensitivity= 84.9% Specificity= 94%
Gupta et al. [57]	Colon cancer survival prediction	Deep auto-encoders	SEER statistics	AUC= 0.95
Rajinikanth et al. [58]	Skin Melanoma Segmentation	VGG-UNet	ISIC2016 challenge dataset	-

ACC: Accuracy, AUC: Area under curve

Cancer research statistics between 2014 and 2022 were obtained through a "Google Scholar" search, which proved to be useful. Fig 2, demonstrates the increasing interest in utilizing deep learning for cancer research. It also shows that lung cancer gets better attention than breast cancer. Breast and lung cancer have the highest ratio in this study. All these statistics were collected by Google Scholar on August 23, 2022, at 7 p.m.

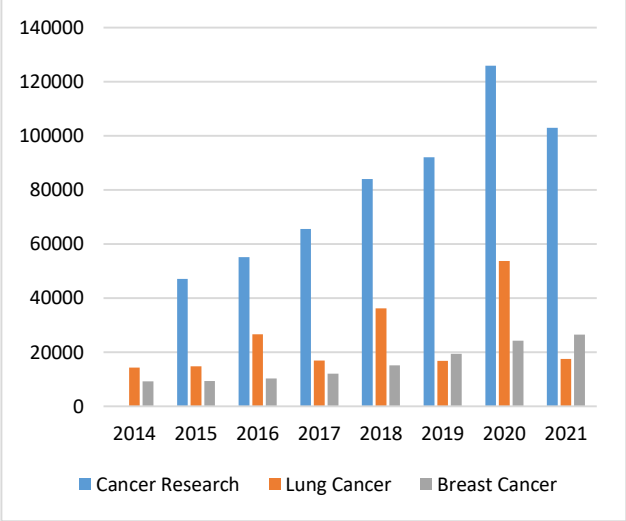

Figure 2. Deep learning cancer research between 2014 and 2022

2024, 21(3): 1101-1118
https://dx.doi.org/10.21123/bsj.2023.8340
P-ISSN: 2078-8665 - E-ISSN: 2411-7986
Baghdad Science Journal

Related work summary

Table 3 illustrates that there are some gaps in the previous studies. The low accuracy in some studies is due to unsuitable methods or inappropriate parameter selection. Some studies used highly computational models. Most studies used one or two performance metrics, which are not sufficient to judge the models and evaluate their performance. However, in the current study, advantage of ensemble learning and transfer learning and the low-computational efficiency of some specific deep models will be taken into account in order to achieve good performance with a low-computational model.

Materials and Methods

Convolutional Neural Network (CNN)

CNN is a deep neural network that accepts its input as a 2D image and produces classes or class probabilities as an output. CNN can be used in many applications, like medical disease diagnosis, human recognition, image classification, etc. [30, 59]. Fig 3 illustrates the architecture of CNN, which includes the convolution layers, the pooling layers, and the fully connected layer.

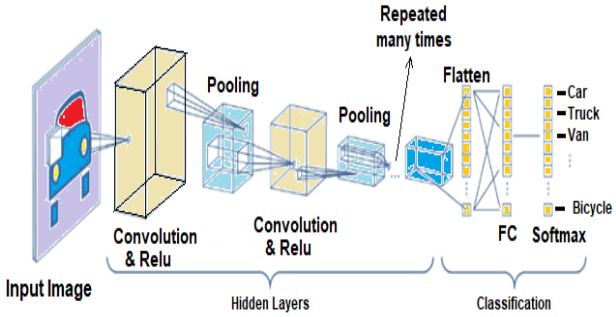

Figure 3. CNN architecture

The convolutional layer applies the convolution process in which the image of size M*N is convolved using a kernel of a specific size K*K. The kernel slides on the image starting from the left upper corner to the lower right corner. Each pixel's neighborhood is defined and multiplied by the kernel pixels, and the sum of the multiplication is used as the result of the convolution. The output of the convolutional layer is called the activation map; whose size differs according to the number of filters.

The convolution process is used in the convolutional layer, which takes an image of size M*N and combines it with a kernel of size K*K. The kernel slides on the image starting from the left upper corner to the lower right corner. The neighborhood of each pixel is defined and multiplied by the kernel pixels, and the sum of the multiplication is used as the result of the convolution. The output of the convolutional layer is called the activation map; whose size differs according to the number of filters. Many parameters define the final convolution size, including the stride and padding. While stride (S) represents the size of the sliding window (kernel), the padding (P) refers to the number of rows and columns that are added to convolve the boundary pixels. For example, if the kernel is of size 5*5, the padding will be 2 (add 2 columns and 2 rows). If the kernel size is 7*7, the padding will be 3. The output size of the convolution layer is calculated as (W-F+2P)/s+1, where W is the size of the image, F is the size of the kernel, S is the stride, and P is the padding. The output of the convolution layer is then moved to the pooling layer, in which the image is reduced by a specific rate. Two different pooling methods can be used in CNN: max pooling and the average pooling. Average pooling takes the average of pooled pixels, while the max pooling takes their maximum value.

The Fully Connected Layer (FC) is connected to all the neurons in the previous layer. The sums of all the weighted products of all the neurons of the previous layer constitute one value of a neuron in this layer. In standard CNN networks, a combination of convolution and pooling layers is used, and then a non-linear activation function is used to eliminate the noisy pixels. Many activation functions can be used, like Sigmoid, Tanh, and RelU. These functions are used after each convolutional layer and before the pooling layer. A flattening layer is usually used before the FC layer in order to rearrange the final convolution results to be consistent with the FC layer.

Proposed transfer learning models

In the current study, three types of CNN architectures that are already pertained models are used. The three models chosen are ResNet50, ResNet101, and EfficientNetB3 because of their efficiency and high performance in image classification. Transfer learning is the concept of using previously trained models for a new problem that is somehow different from the original problem, as shown in Fig. 4-A. ResNets and

2024, 21(3): 1101-1118
https://dx.doi.org/10.21123/bsj.2023.8340
P-ISSN: 2078-8665 - E-ISSN: 2411-7986
Baghdad Science Journal

EfficientNet models are already trained on the ImageNet dataset. In this study, these models will be used for lung cancer prediction.

ResNet50 is another type of CNN that uses the residual units that were first invented by He et al.[31]. ResNet50 is a 50-layer deep network consisting of 48 convolutional layers, one max pooling layer and one FC layer. The main advantage of ResNet50 is the residual units. Residual units eliminate the problem of vanishing gradient, from which the previous deep networks suffered. The ResNet50 architecture includes the residual units in all parts; they work as skipping connections (as shown in Fig 4-B).

By going deeper, the gradient minimizes, and after going too deep, the gradient becomes very small or vanishes. In the ResNet architecture and by using the residual units, there will be connections skipping two or more convolutional layers (3 in ResNet50) preventing the gradient from vanishing.

The architecture of the ResNet50 consists of 50 convolutional layers starting with a convolutional layer of 64 filters of size 7*7 using a stride of 2. The next layer is the max pooling layer (stride = 2) to minimize the convolution size. After that, there are three convolution layers with 64 filters of size 1*1, followed by 64 filters of size 3*3, and 256 filters of size 1*1. The next four convolutional layers consist of 128 filters of size 1*1, followed by 128 filters of size 3*3, and 512 filters of size 1*1. The next layer has 256 filters of size 1*1, followed by 256 filters of size 3*3, and 1024 filters of size 1*1 (this combination is repeated 6 times). The final convolution layers contain 512 filters of size 1*1, 512 filters of size 3*3, and 2048 filters of size 1*1. The final layer of the ResNet50 is the FC layer, or the average pooling layer which includes 1000 samples (the final feature vector) with a "Softmax" activation function to classify the image into the corresponding class. RenNet101, on the other hand, has 101 layers and is trained on the ImageNet dataset. It includes 44.5 million training parameters.

Tan and Quoc [33] proposed the idea of EfficientNet based on CNN architecture and the concept of scaling all dimensions (depth, width and resolution) using the compound coefficients. As a result, they created a family of EfficientNet architectures with high accuracy and smaller size. EfficientNet proved its computational efficiency which exceeded all other previous models (ResNets, Xception, NasNet, Inception, etc.). Compound scaling (Fig 4-C) is used to uniformly scale the three dimensions of the network, allowing the model to act in a dynamic way according to the input size (the bigger the input size, the deeper the network).

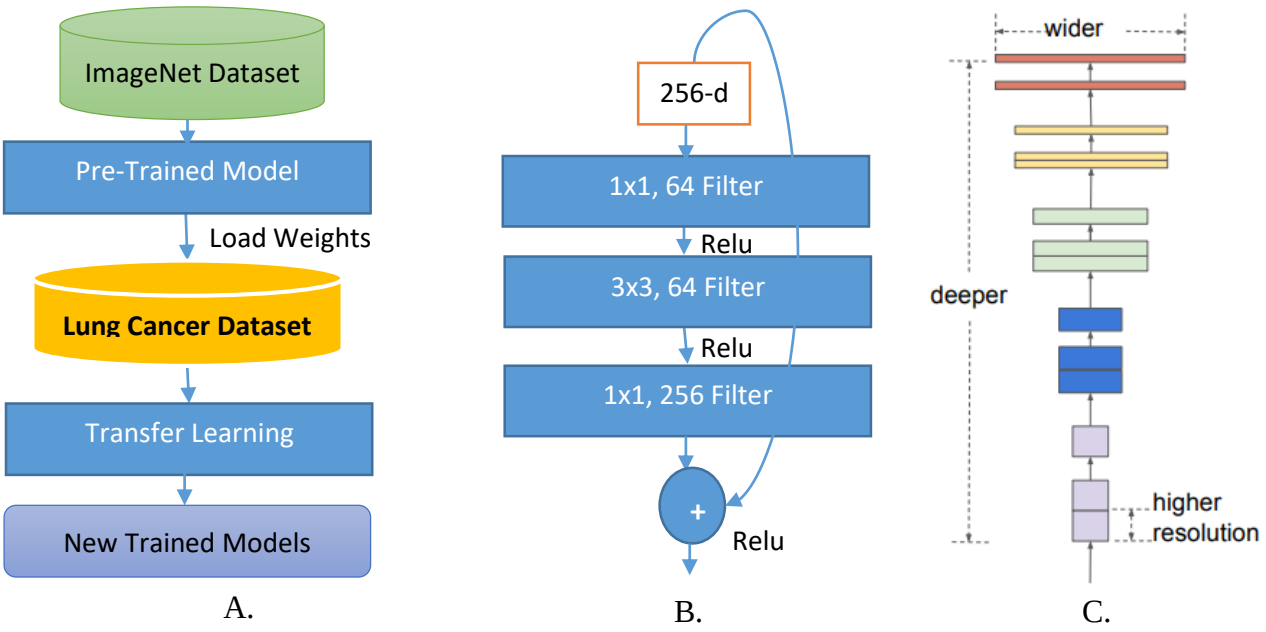

A. B. C.

Figure 4. Deep network main concept: A) Transfer learning concept, B) Residual unit of ResNet50 network, C) EfficientNet compound scaling concept

Dataset

2024, 21(3): 1101-1118
https://dx.doi.org/10.21123/bsj.2023.8340
P-ISSN: 2078-8665 - E-ISSN: 2411-7986
Baghdad Science Journal

The chosen dataset is the Chest CT-Scan images dataset available from Kaggle[60].The dataset consists of three separate folders: the training dataset, the validation dataset and the test dataset with a separation ratio of (70% for train, 20% for validation and 10% for testing). The training dataset includes 613 images, 315 images and 72 images for training, validation and testing, respectively.

The dataset is used to classify lung cancer into different categories (which is the main challenge of this dataset). There are 4 different classes in this dataset, including adenocarcinoma, large cell carcinoma, squamous cell carcinoma and the normal case.

Fig 5, displays examples of the training dataset from various categories and illustrates the similarity between them (such as adenocarcinoma and large cells), so distinguishing between those two types requires a robust classifier (which is the main reason for choosing deep learning). The similarity between classes is the main challenge of this dataset. However, its size is low, and to address this problem, the data augmentation process will be used.

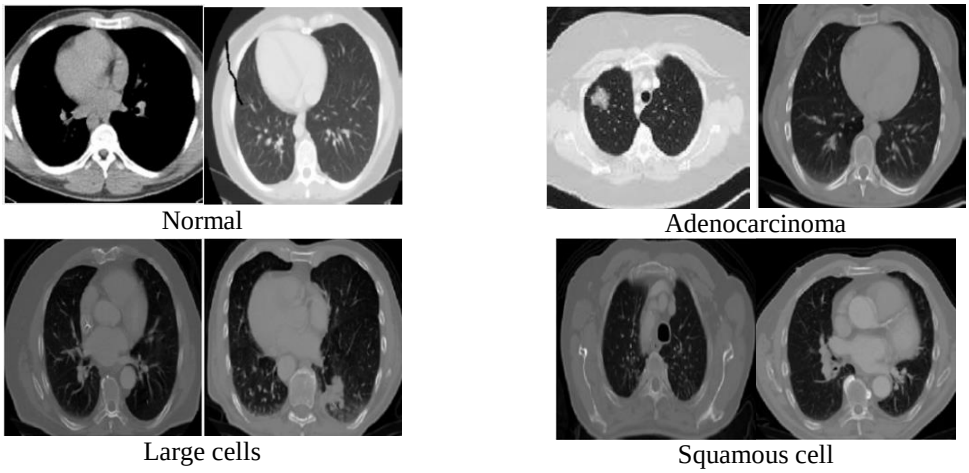

Figure 5. Examples of the three types of lung cancer and the normal case

Results and discussion

Proposed architecture and parameter selection

The main steps of the lung cancer diagnosis system are described in Fig. 6. First, the lung CT image dataset is obtained. To be consistent with the input layer of the deep learning networks used, the training, validation, and test sets are pre-processed using many image processing steps, including RGB conversion and resizing into 224*224. The training set is also manipulated using the data augmentation step, which rotates, flips, and zooms the lung CT image to obtain different versions of the same CT image (this step aims to increase the number of training images and learn the model on different degradation levels of the same image, which can prevent overfitting and improve the training stage). Flipping is applied using horizontal flipping, zooming is applied using a zoom range of 0.05, and rotation is applied using a rotation range of 0.05. The training and validation sets are then fed into three different models (ResNet50, ResNet101 and EffecientNetB3). The reason for choosing these models is their efficiency in image classification tasks (EffecientNetB3, ResNet50 and ResNet101 are very common types of deep models as Table 2 shows). EffecientNetB3 is considered a low-computational deep model. The transfer learning approach is applied in order to retrain the same deep learning pre-trained models on a specific problem (The lung cancer diagnosis problem). The transfer learning will be applied with extra layers to the deep network architecture.

The architecture of the three proposed deep learning models includes the following layers:

1. The base model (which will be one of the following: (ResNet50, ResNet101, EfficientNetB3)).
2. Batch normalization layer
3. Dense layer (fully connected layer) with 256 neurons, and 'Relu' activation function.
4. Dropout layer with a dropout rate of 35%.
5. Classification layer (Dense layer) with 4 neurons representing the targets, and a 'Softmax' activation function.

The selected training parameters are:

2024, 21(3): 1101-1118
https://dx.doi.org/10.21123/bsj.2023.8340
P-ISSN: 2078-8665 - E-ISSN: 2411-7986
Baghdad Science Journal

- All models will be compiled using the Adam optimizer (learning rate of 0.01).
- The categorical cross-entropy loss function is used (since the problem is a multi-class classification problem).
- The accuracy is chosen as the performance metric.
- The used batch size is 50.
- The patience factor is 5 (the number of epochs to wait before stopping the training process if the monitored metric does not improve). The monitored metric is validation accuracy.
- The reduction factor for the learning rate is 0.5.

The performance evaluation process includes computing the training accuracy, validation accuracy, test accuracy, training loss, validation loss, test loss, training time per epoch, precision, recall, and F1-score.

After training the three different models, transfer ensemble learning is used to fuse the trained models together in order to get the best performance of all models. The stacking method is used, and the performance of the resulting deep ensemble models is evaluated.

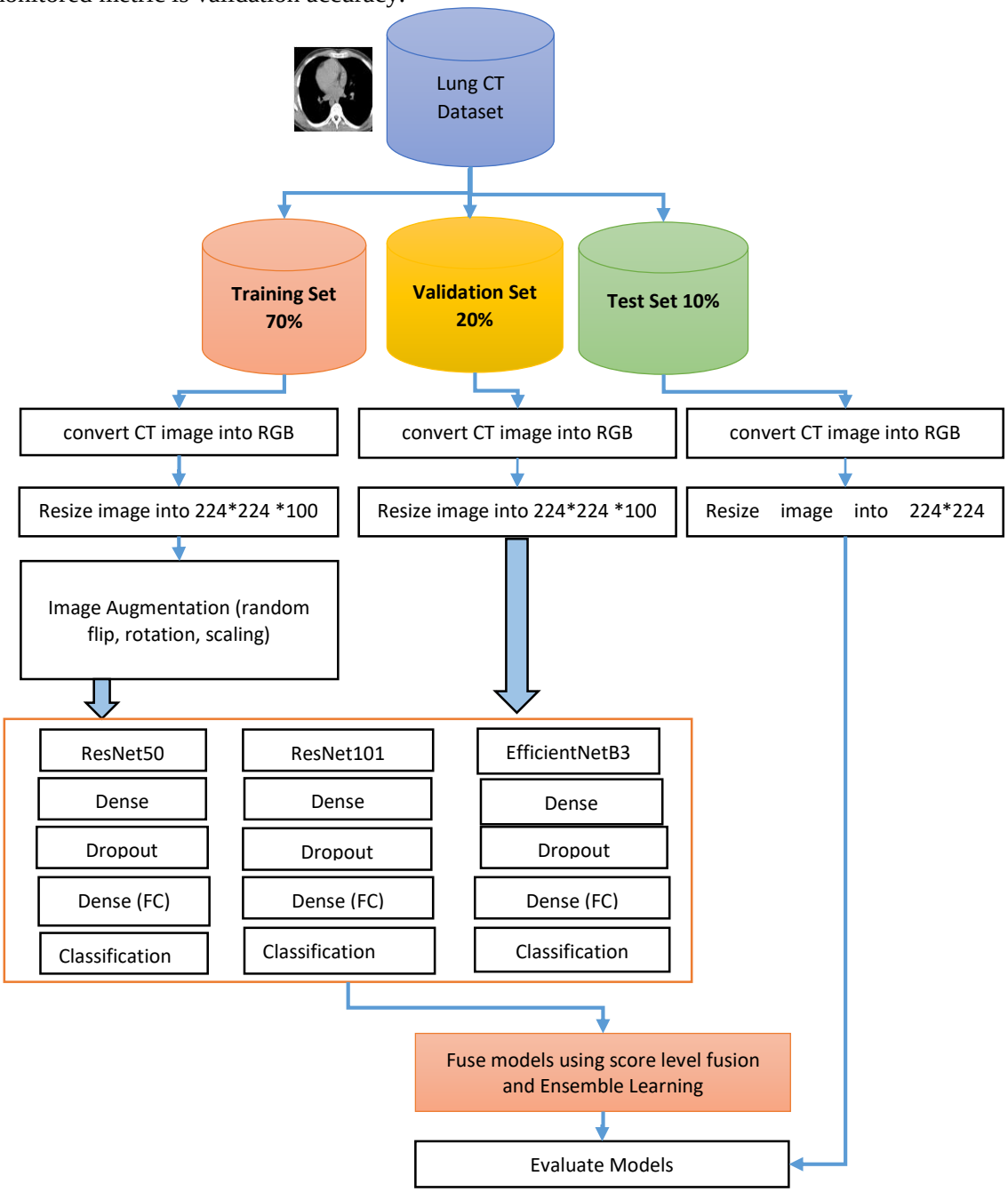

Figure 6. Main steps of the proposed lung cancer diagnosis system.

2024, 21(3): 1101-1118
https://dx.doi.org/10.21123/bsj.2023.8340
P-ISSN: 2078-8665 - E-ISSN: 2411-7986
Baghdad Science Journal

Proposed training scenarios

The previous experimental part leads us to the following training and evaluation scenarios:

1. Training ResNet50-Dense-Dropout model using the training set and evaluating it using the evaluation set.
2. Test the trained ResNet50-Dense-Dropout model using the test set and evaluation metrics.
3. Training the ResNet101-Dense-Dropout model using the training set and evaluating it using the evaluation set.
4. Test the trained ResNet101-Dense-Dropout model using the test set and evaluation metrics.
5. Training the EfficientB3-Dense-Dropout model using the training set and evaluating it using the evaluation set.
6. Test the trained EfficientB3-Dense-Dropout model using the test set and evaluation metrics.
7. Apply score level fusion of the three trained models and evaluate the fused model.
8. Build an ensemble of ResNet50-Dense-Dropout, ResNet101-Dense-Dropout, and EfficientB3-Dense-Dropout models using the stacking ensemble approach.
9. Test the trained ensemble model using the test set and evaluation metrics.

Experimental results

All models are trained according to those previous scenarios. The training and validation accuracy, along with the training and validation loss, is computed through the training epochs. The best validation value for each scenario is also computed. Fig 7 shows the accuracy and loss curves. For the EffiecientNetB3 model, the best epochs are 40 and 32 in terms of loss and accuracy, respectively. The best epoch for the ResNet5o model is 15 for both accuracy and loss. The best epochs for the ResNet101 model are 14 and 15 for accuracy and loss, respectively.

A.

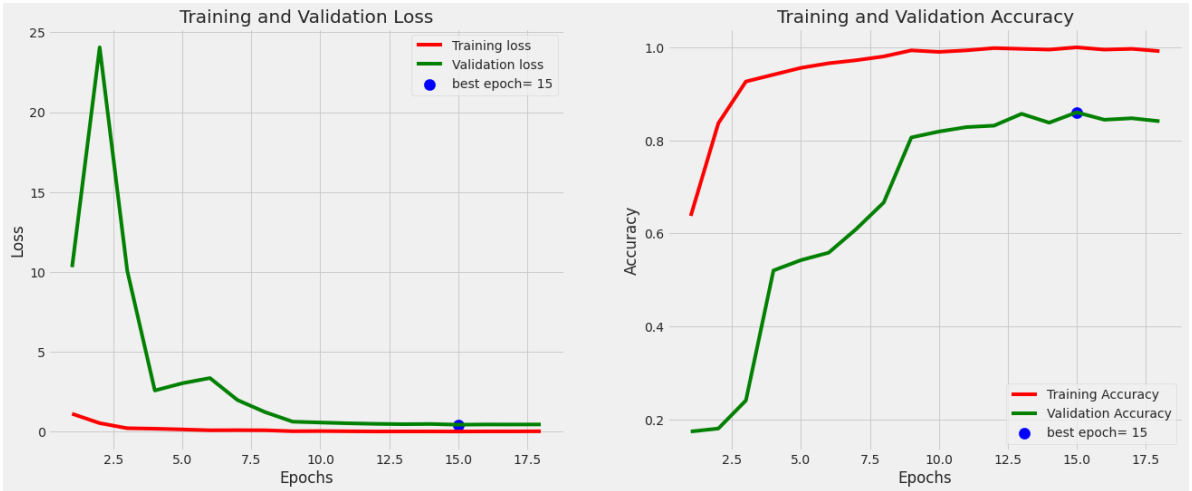

B.

2024, 21(3): 1101-1118
https://dx.doi.org/10.21123/bsj.2023.8340
P-ISSN: 2078-8665 - E-ISSN: 2411-7986
Baghdad Science Journal

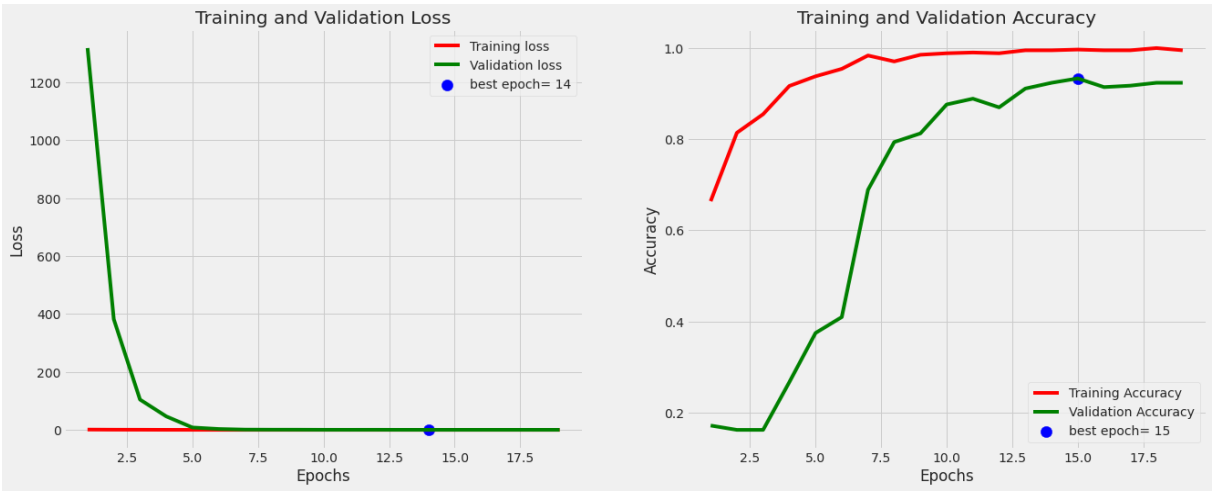

C.

Figure 7. Training and validation accuracy and loss curves: A) EffiecientNetB3-Dense-Dropout, B) ResNet50-Dense-Dropout, C) ResNet101-Dense-Dropout

Fig 7 shows that EfficientNetB3 is the best-trained model with the best convergence. The EfficientNetB3 achieved 97.5% training accuracy, 94.99% validation accuracy and 93.05% test accuracy. However, the ResNet50 model got 97.5%, 75% and 80.55% as training, validation and test accuracy, respectively. The ResNet101 models achieved 100%, 94.99% and 93.05% as training, validation and test accuracy, respectively. The least training, validation and test loss was corresponding to the ResNet101 model, with 0.0003 for training, 0.11 for validation and 0.47 for the test. Fig 8-A to 8-D show the detailed confusion matrix computations of the three trained models and the score-level fusion one.

Fig 8 shows that the EfficientNetB3 model has the best results compared to all individual models since the main axis of the confusion matrix includes most of the hits. The number of false positives and false negatives is also lower than the corresponding values in other models. However, the score-level fusion gives very similar results.

Fig 8 illustrates that the EfficientNetB3 model and the fused model preserve the same performance, which is better than individual ResNet models. However, a detailed performance comparison between all models for the four categories is presented in Table 4.

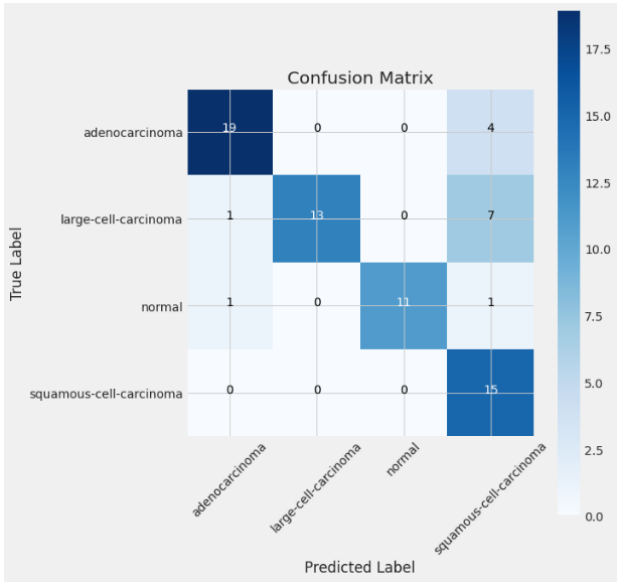

A.

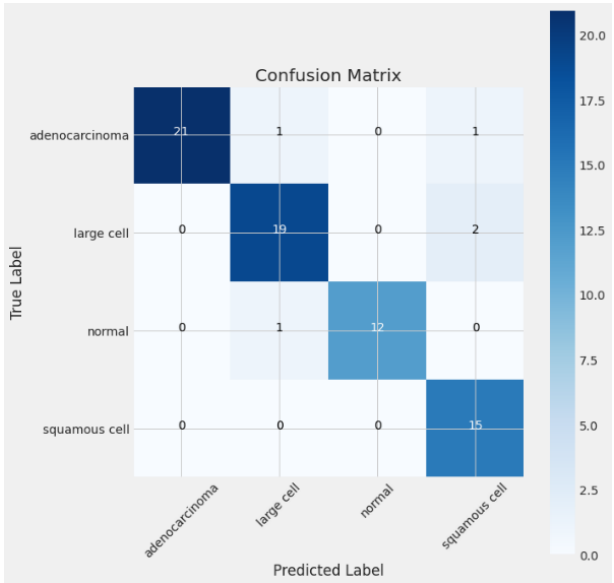

B.

2024, 21(3): 1101-1118
https://dx.doi.org/10.21123/bsj.2023.8340
P-ISSN: 2078-8665 - E-ISSN: 2411-7986
Baghdad Science Journal

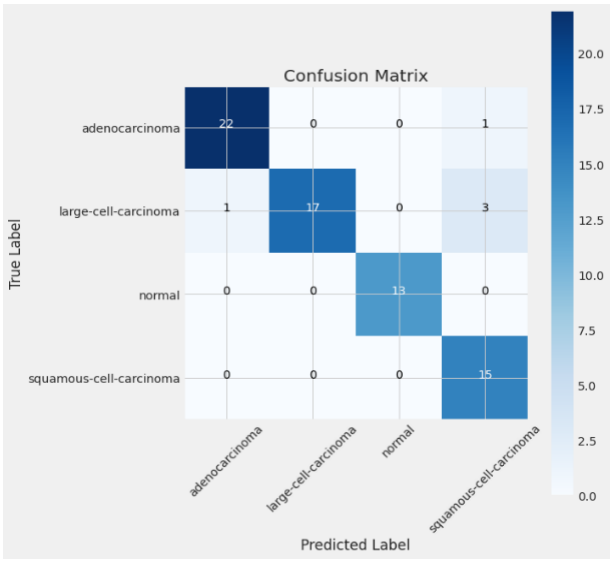

C.

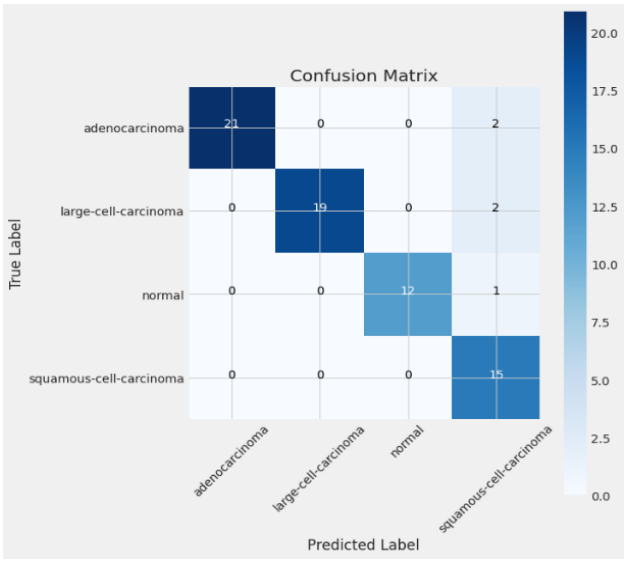

D.

Figure 8. Confusion Matrix of the trained models: A) EffiecientNetB3-Dense-Dropout model, B) ResNet50-Dense-Dropout model, C) ResNet101-Dense-Dropout model, D) Score level fusion of ResNet and EffecientNetB3

Table 4. Precision, recall and F1-score evaluation metrics for all trained models.

Model	Precision				
	adenocarcinoma	***large-cell***	***Normal***	***Squamous cell***	***Average Value***
EffiecientNetB3-Dense-Dropout	**100**	90	**100**	**83**	94
ResNet50-Dense-Dropout	90	**100**	**100**	56	88
ResNet101-Dense-Dropout	96	**100**	**100**	79	94
Score-level fusion model	**100**	**100**	**100**	75	**95**
Model	Recall				
	adenocarcinoma	***large-cell***	***Normal***	***Squamous cell***	***Average Value***
EffiecientNetB3-Dense-Dropout	91	**90**	92	**100**	**93**
ResNet50-Dense-Dropout	83	62	85	**100**	81
ResNet101-Dense-Dropout	**96**	81	**100**	**100**	**93**
Score-level fusion model	91	**90**	92	**100**	**93**
Model	F1-Score				
	adenocarcinoma	***large-cell***	***Normal***	***Squamous cell***	***Average Value***
EffiecientNetB3-Dense-Dropout	**95**	90	**96**	**91**	**93**
ResNet50-Dense-Dropout	86	76	92	71	81
ResNet101-Dense-Dropout	**96**	89	**100**	88	93
Score-level fusion model	**95**	**95**	**96**	86	**93**

Table 4 proves that the EffiecientNetB3-Dense-Dropout model achieves the best results with 94% average accuracy. However, using the score-level fusion of all models increased the precision value by 1%, whenever the recall and F1-score remained the same. Table 4 also proves that the best class precision corresponds with the "Normal" class. The best recall value is related to the "Squamous" class, while the "Normal" class achieves the best F1-score. In all practical scenarios, the performance of ResNet101 is better than the corresponding performance of ResNet50. Table 5 includes a comparison between the original models and the ensemble model accuracies. From a "time" computation point of view, the ResNet50 consumed almost 12.49 seconds per epoch, the ResNet101 needed almost 15.41 seconds per epoch, and the average training time of each epoch in the EfficientNetB3 model was almost 15.32 seconds.

Table 5. Comparison between individual models, fused model, and the ensemble model accuracies.

Model	Validation Accuracy %
EffiecientNetB3-Dense-Dropout	93
ResNet50-Dense-Dropout	81
ResNet101-Dense-Dropout	93
Score-level fusion model	93
Ensemble Model	99.44

2024, 21(3): 1101-1118
https://dx.doi.org/10.21123/bsj.2023.8340
P-ISSN: 2078-8665 - E-ISSN: 2411-7986
Baghdad Science Journal

Table 5 proves that the ensemble model has the best validation accuracy (99.44%) with an enhancement of 6.44% compared to the EfficientNetB3 and ResNet101 models. However, the ensemble model performance exceeds the performance of ResNet50 by 18.44%. The efficientNetB3 and ResNet101 models have similar validation accuracy, which is also the same for the fused model. However, making an ensemble of all these individual models achieves a validation accuracy of 99.44%. Table 6 includes a comparison between the proposed methods and the related work. The comparison proves the high performance and efficiency of the current system among other state-of-the-art studies.

Table 6. Comparison between the current study and the related state-of-the-art studies.

Study	Field description	DL model	Dataset	Results
Xu et al [39]	Skin cancer prediction	AlexNet, VGG16 and ResNet-18	150 validation images of the ISIC challenge	AUC= 83.83% for melanoma. AUC= 97.55% for seborrheic keratosis
Alakwaa et al. [19]	Lung cancer detection	3DCNN	Images of 1397 patients of DSB dataset	ACC=86.6%
Benhammou et al. [20]	Breast cancer detection	CNN	7909 cases of BreakHis dataset	ACC=88.9%
Xie et al. [44]	Pulmonary nodule detection	R-CNN, 2D CNN	LUNA-16	ACC=86.4%
Coudray et al. [45]	Non-small Lung cancer detection	Inception V3	1634 lung images	ACC=85.6%
Mahdi [61]	Leukemia Cancer detection	SGD-SVM	Two datasets (The first contains 50 samples, the second contains 100 samples)	First dataset: Specificity 94.4%, sensitivity: 75% Second dataset: specificity: 80%, sensitivity: 74.54%
Hasan et al. [62]	Breast Cancer MRI Classification	CNN	652 images	ACC= 98.77%
Current Study	Lung cancer detection and classification (adenocarcinoma, large cell carcinoma, squamous cell carcinoma, normal)	Ensemble transfer learning, score-level fusion, EfficientNetB3, ResNet50 and ResNet101	1000 images of Kaggle lung cancer dataset	Best Individual accuracy (EfficientNet 93%) Fusion ACC=99.44%

Limitations

Despite the improvement in lung cancer prediction provided by the current study, there are some limitations, including the use of small data sizes and the use of specific pertained models. Lung images need some preprocessing steps like image segmentation in order to extract the region of interest (ROI) or lung tissues.

Conclusion

The current research introduced theoretical and practical studies of cancer-related deep-learning methodologies. The theoretical part introduces an analysis and comparative study of the previous deep-learning cancer-related research. Many different types of cancer are also considered (lung, breast, colon, stomach, brain, skin, and so on). The study also compares different types of cancer datasets and their contributions to cancer research. Cancer prediction, cancer prevention, cancer diagnosis, cancer classification, and many other applications of deep learning models are also studied and discussed.

To address the problem of the low accuracy of the current lung cancer prediction systems, a new ensemble transfer learning and score-level fusion of three powerful deep learning architectures was implemented and tested. Ensemble learning was chosen in order to improve the performance of lung cancer prediction systems. A multi-class dataset,

2024, 21(3): 1101-1118
https://dx.doi.org/10.21123/bsj.2023.8340
P-ISSN: 2078-8665 - E-ISSN: 2411-7986
Baghdad Science Journal

including four different classes, was suggested in order to make the trained model more reliable.

In the first step, the CT lung image dataset was pre-processed and the data augmentation process was applied in order to increase the dataset. Then, three different deep learning architectures were designed based on the EfficientNetB3, ResNet50 and ResNet101 models. The dense layers, dropout layers and classification layers were also added to each individual model. The training set (70% of the entire data) and the validation set (20% of the entire data) were used to train and validate the three models. After that, the score level fusion was used to fuse the decisions of the three models. Finally, an ensemble of the three models was built and trained using the stacking methodology.

Experiments show that ResNet101 and EfficientNetB3 have similar performance in all training scenarios. However, ResNet59 has a lower accuracy. The score-level fusion increased some lung cancer class accuracy but the overall accuracy was almost the same as EfficientNetB3. The ensemble learning increased the accuracy by 6.44%.

Future studies can benefit from the theoretical comparison of the cancer deep models. This information can be used as a guide for future studies. The practical study can also be used by physicians as a medical support tool for the prediction of lung cancer based on CT scan images.

The current study's main limitation is the small data size. Lung images need some preprocessing steps to extract the ROI of lung tissues.

In future work, other deep learning models can be used in the same ensemble, and their performances can be compared. The next study can also focus on increasing the data size and comparing the current methodology to other types of cancer. Other future work can focus on applying some preprocessing steps like image segmentation in order to concentrate the deep learning on the effective parts of images and not the entire image.

Author's Declaration

- Conflicts of Interest: None.
- We hereby confirm that all the Figures and Tables in the manuscript are ours. Furthermore, any Figures and images that are not ours have been included with the necessary permission for re-publication, which is attached to the manuscript.
- Authors sign on ethical consideration's approval.
- Ethical Clearance: The project was approved by the local ethical committee in University of Al Hikma University College.

Author's Contribution

O. A. J., M. J. A., and Z. H. S. participated in configuring the idea of the paper. O. A. J. collected the dataset and configured the final folders of each category. M. J. A. designed the models, including the architecture of the deep learning networks. Z. H. S. implemented the design along with O.A.J. All authors participated in the writing part.

References

1. Chugh G, Kumar S, Singh N. Survey on machine learning and deep learning applications in breast cancer diagnosis. Cognit Comput. 2021 Jan:1-20. https://doi.org/10.1007/s12559-020-09813-6
2. Aljuaid H, Alturki N, Alsubaie N, Cavallaro L, Liotta A. Computer-aided diagnosis for breast cancer classification using deep neural networks and transfer learning. Comput. Methods Programs Biomed. 2022 Aug 1; 223: 106951. https://doi.org/10.1016/j.cmpb.2022.106951
3. World Health Organization, WHO position paper on mammography screening, Geneva, Switzerland: WHO Library Cataloguing-in-Publication Data, 2014. https://apps.who.int/iris/bitstream/handle/10665/137339/?sequence=1
4. International Agency for Research on Cancer, "The Global Cancer Burden in 2018- framing global cancer control," International Agency for Research on Cancer, Kuala Lumpur - Malaysia, 2018. https://pesquisa.bvsalud.org/portal/resource/pt/lis-46560?src=similardocs&utm_medium=email&utm_source=transaction
5. American Cancer Society, "Cancer facts and figures 2019," American Cancer Society, 2019. https://www.cancer.org/research/cancer-facts-statistics/all-cancer-facts-figures/cancer-facts-figures-2019.html

6. world bladder cancer, "GLOBOCAN 2020: Bladder cancer 10th most commonly diagnosed worldwide," world bladder cancer, Lyon , France, 2020. https://worldbladdercancer.org/news_events/globocan-2020-bladder-cancer-10th-most-commonly-diagnosed-worldwide/
7. American Cancer Society, "Cancer Facts & Figures 2021," American Cancer Society, 2021. https://www.cancer.org/research/cancer-facts-statistics/all-cancer-facts-figures/cancer-facts-figures-2021.html
8. American Cancer Society, "Cancer Facts & Figures 2022," American Cancer Society, 2022. https://www.cancer.org/research/cancer-facts-statistics/all-cancer-facts-figures/cancer-facts-figures-2022.html
9. Sung H, Ferlay J, Siegel RL, Laversanne M, Soerjomataram I, Jemal A, et al. Global cancer statistics 2020: GLOBOCAN estimates of incidence and mortality worldwide for 36 cancers in 185 countries. CA Cancer J Clin. 2021 May; 71(3): 209-49. https://doi.org/10.3322/caac.21660
10. Survarachakan S, Prasad PJ, Naseem R, Frutos JP, Kumar RP, Langø T, et al. Deep learning for image-based liver analysis—A comprehensive review focusing on malignant lesions. Artif Intell Med.. 2022 Jun 9; 130: 102331. https://doi.org/10.1016/j.artmed.2022.102331
11. American Cancer Society, "Cancer Facts & Figures 2023," American Cancer Society, Atlanta, 2023. https://www.cancer.org/research/cancer-facts-statistics/all-cancer-facts-figures/2023-cancer-facts-figures.html
12. Ravì D, Wong C, Deligianni F, Berthelot M, Andreu-Perez J, Lo B, et al. Deep learning for health informatics. IEEE J Biomed Health Inf. 2016 Dec 29;21(1):4-21. https://doi.org/10.1109/JBHI.2016.2636665
13. Triantafyllidis A, Kondylakis H, Katehakis D, Kouroubali A, Koumakis L, Marias K, et al. Deep learning in mHealth for cardiovascular disease, diabetes, and cancer: systematic review. JMIR mHealth and uHealth. 2022 Apr 4; 10(4): e32344. https://doi.org/10.2196/32344
14. Mohammed MA, Abdulkareem KH, Dinar AM, Zapirain BG. Rise of Deep Learning Clinical Applications and Challenges in Omics Data: A Systematic Review. Diagnostics. 2023 Feb 10; 13(4): 664. https://doi.org/10.3390/diagnostics13040664
15. Mukhlif AA, Al-Khateeb B, Mohammed MA. Incorporating a Novel Dual Transfer Learning Approach for Medical Images. Sensors. 2023 Jan; 23(2): 570. https://doi.org/10.3390/s23020570
16. Ahmad AS, Mayya AM. A new tool to predict lung cancer based on risk factors. Heliyon. 2020 Feb 1; 6(2): e03402. https://doi.org/10.1016/j.heliyon.2020.e03402
17. Dalmiglio C, Brilli L, Campanile M, Ciuoli C, Cartocci A, Castagna MG. CONUT score: a new tool for predicting prognosis in patients with advanced thyroid cancer treated with TKI. Cancers. 2022 Jan 30; 14(3): 724. https://doi.org/10.3390/cancers14030724
18. Huang C, Su Q, Ding Z, Zeng W, Zhou Z. A novel clinical tool to predict cancer-specific survival in patients with primary pelvic sarcomas: A large population-based retrospective cohort study. Cancer Med. 2023 Jan; 12(2): 1279-92. https://doi.org/10.1002/cam4.4998, https://doi.org/10.3390/ijms23031809
19. Asuntha A, Srinivasan A. Deep learning for lung Cancer detection and classification. Multimedia Tools Appl. 2020 Mar;79: 7731-62. https://doi.org/10.1007/s11042-019-08394-3
20. Benhammou Y, Achchab B, Herrera F, Tabik S. BreakHis based breast cancer automatic diagnosis using deep learning: Taxonomy, survey and insights. Neurocomputing. 2020 Jan 29; 375: 9-24. https://doi.org/10.1016/j.neucom.2019.09.044
21. Yurttakal AH, Erbay H, İkizceli T, Karaçavuş S. Detection of breast cancer via deep convolution neural networks using MRI images. Multimedia Tools Appl. 2020 Jun;79: 15555-73. https://doi.org/10.1007/s11042-019-7479-6
22. Liu T, Siegel E, Shen D. Deep learning and medical image analysis for COVID-19 diagnosis and prediction. Annu Rev Biomed Eng. 2022 Jun 6; 24: 179-201. https://doi.org/10.1146/annurev-bioeng-110220-012203
23. Mayya A, Khozama S. A Novel Medical Support Deep Learning Fusion Model for the Diagnosis of COVID-19. IEEE Int Conf. Adv Trends Multi-Discip. Res Innovation. 2020 Dec 30 (pp. 1-6). IEEE. https://doi.org/10.1109/ICATMRI51801.2020.9398317
24. Kondaveeti HK, Edupuganti P. Skin cancer classification using transfer learning. In2020 IEEE Int. Conf. Advent Trends in Multi-Discip. Res Innovation. 2020 Dec 30 (pp. 1-4). IEEE. https://doi.org/10.1109/ICATMRI51801.2020.9398388
25. Ma Q, Xu D. Deep learning shapes single-cell data analysis. Nat Rev Mol Cell Biol. 2022 May; 23(5): 303-4. https://doi.org/10.1038/s41580-022-00466-x
26. Nagarajan SM, Deverajan GG, Chatterjee P, Alnumay W, Ghosh U. Effective task scheduling algorithm with deep learning for Internet of Health Things (IoHT). Sustain Cities Soc. 2021 Aug 1;71:102945. https://doi.org/10.1016/j.scs.2021.102945
27. Lavanya PM, Sasikala E. Deep learning techniques on text classification using Natural language processing (NLP) in social healthcare network: A comprehensive survey. 3rd Int. Conf Signal Process

Commun. 2021 May 13 (pp. 603-609). IEEE. https://doi.org/10.1109/ICSPC51351.2021.9451752
28. Hinton GE, Salakhutdinov RR. Reducing the dimensionality of data with neural networks. Science. 2006 Jul 28; 313(5786): 504-7. https://doi.org/10.1126/science.1127647
29. Hinton GE, Osindero S, Teh YW. A fast learning algorithm for deep belief nets. Neural comput. 2006 Jul 1; 18(7): 1527-54. https://doi.org/10.1162/neco.2006.18.7.1527
30. Sarvamangala DR, Kulkarni RV. Convolutional neural networks in medical image understanding: a survey. Evol Intell. 2022 Mar; 15(1): 1-22. https://doi.org/10.1007/s12065-020-00540-3.
31. He K, Zhang X, Ren S, Sun J. Deep residual learning for image recognition. Proc IEEE Comput Soc Conf Comput Vis Pattern Recognit. 2016 (pp. 770-778). https://openaccess.thecvf.com/content_cvpr_2016/html/He_Deep_Residual_Learning_CVPR_2016_paper.html
32. Szegedy C, Liu W, Jia Y, Sermanet P, Reed S, Anguelov D, et al. Going deeper with convolutions. Proc IEEE Comput Vis Pattern Recognit. 2015 (pp. 1-9). https://www.cv-foundation.org/openaccess/content_cvpr_2015/html/Szegedy_Going_Deeper_With_2015_CVPR_paper.html
33. Tan M, Le Q. Efficientnet: Rethinking model scaling for convolutional neural networks. Proc 36th Int Conf Mach Learn. 2019 May 24 (pp. 6105-6114). PMLR. http://proceedings.mlr.press/v97/tan19a.html
34. Bhatt C, Kumar I, Vijayakumar V, Singh KU, Kumar A. The state of the art of deep learning models in medical science and their challenges. Multimedia Syst. 2021 Aug; 27(4): 599-613. https://doi.org/10.1007/s00530-020-00694-1
35. Cao C, Liu F, Tan H, Song D, Shu W, Li W, et al. Deep learning and its applications in biomedicine. Genom Proteom Bioinform. 2018 Feb 1; 16(1): 17-32. https://doi.org/10.1016/j.gpb.2017.07.003
36. Selvathi D, Aarthy Poornila A. Deep learning techniques for breast cancer detection using medical image analysis. Biol. rationalized Comput. Tech Image Proc Appl. 2018: 159-86. https://doi.org/10.1007/978-3-319-61316-1_8
37. Khan S, Islam N, Jan Z, Din IU, Rodrigues JJ. A novel deep learning based framework for the detection and classification of breast cancer using transfer learning. Pattern Recognit Lett. 2019 Jul 1; 125: 1-6. https://doi.org/10.1016/j.patrec.2019.03.022
38. Mukhlif AA, Al-Khateeb B, Mohammed M. Classification of breast cancer images using new transfer learning techniques. Iraqi J Comput Sci Math. 2023 Jan 7; 4(1): 167-80. https://doi.org/10.52866/ijcsm.2023.01.01.0014
39. Mahbod A, Schaefer G, Wang C, Ecker R, Ellinge I. Skin lesion classification using hybrid deep neural networks. IEEE Int Conf Acoust Speech Signal Process 2019 May 12 (pp. 1229-1233). IEEE. https://doi.org/10.1109/ICASSP.2019.8683352
40. Samala RK, Chan HP, Hadjiiski L, Helvie MA, Richter CD, Cha KH. Breast cancer diagnosis in digital breast tomosynthesis: effects of training sample size on multi-stage transfer learning using deep neural nets. IEEE Trans Med Imaging. 2018 Sep 16; 38(3): 686-96. https://doi.org/10.1109/TMI.2018.2870343
41. Li X, Qin G, He Q, Sun L, Zeng H, He Z, et al. Digital breast tomosynthesis versus digital mammography: integration of image modalities enhances deep learning-based breast mass classification. Eur Radio. 2020 Feb; 30: 778-88. https://doi.org/10.1007/s00330-019-06457-5
42. Nagpal K, Foote D, Liu Y, Chen PH, Wulczyn E, Tan F, et al. Development and validation of a deep learning algorithm for improving Gleason scoring of prostate cancer. J Digital Med. 2019 Jun 7; 2(1): 48. https://doi.org/10.1038/s41746-019-0112-2
43. Ardila D, Kiraly AP, Bharadwaj S, Choi B, Reicher JJ, Peng L, et al. End-to-end lung cancer screening with three-dimensional deep learning on low-dose chest computed tomography. Nat Med. 2019 Jun; 25(6): 954-61. https://doi.org/10.1038/s41591-019-0447-x
44. Xie H, Yang D, Sun N, Chen Z, Zhang Y. Automated pulmonary nodule detection in CT images using deep convolutional neural networks. Pattern Recognit. 2019 Jan 1; 85: 109-19. https://doi.org/10.1016/j.patcog.2018.07.031
45. Coudray N, Ocampo PS, Sakellaropoulos T, Narula N, Snuderl M, Fenyö D, et al. Classification and mutation prediction from non–small cell lung cancer histopathology images using deep learning. Nat Med. 2018 Oct; 24(10): 1559-67. https://doi.org/10.1038/s41591-018-0177-5
46. Ech-Cherif A, Misbhauddin M, Ech-Cherif M. Deep neural network based mobile dermoscopy application for triaging skin cancer detection. 2nd Int. Conf Comput Appl Inf Secur. 2019 May 1 (pp. 1-6). IEEE. https://doi.org/10.1109/CAIS.2019.8769517.
47. Guo P, Xue Z, Mtema Z, Yeates K, Ginsburg O, Demarco M, et al. Ensemble deep learning for cervix image selection toward improving reliability in automated cervical precancer screening. Diagnostics. 2020 Jul 3; 10(7): 451. https://doi.org/10.3390/diagnostics10070451
48. Hu L, Horning MP, Banik D, Ajenifuja OK, Adepiti CA, Yeates K, et al. Deep learning-based image evaluation for cervical precancer screening with a smartphone targeting low resource settings–Engineering approach 42nd Annu Int Conf IEEE Eng Med Biol Soc. 2020 Jul 20 (pp. 1944-1949). IEEE. https://doi.org/10.1109/EMBC44109.2020.9175863
49. Senthilkumar G, Ramakrishnan J, Frnda J, Ramachandran M, Gupta D, Tiwari P, et al.

Incorporating artificial fish swarm in ensemble classification framework for recurrence prediction of cervical cancer. IEEE Access. 2021 Jun 7; 9: 83876-86. https://doi.org/10.1109/ACCESS.2021.3087022
50. Alzubaidi L, Al-Amidie M, Al-Asadi A, Humaidi AJ, Al-Shamma O, Fadhel MA, et al. Novel transfer learning approach for medical imaging with limited labeled data. Cancers. 2021 Mar 30; 13(7): 1590. https://doi.org/10.3390/cancers13071590
51. Ashokkumar N, Meera S, Anandan P, Murthy MY, Kalaivani KS, Alahmadi TA, et al. Deep Learning Mechanism for Predicting the Axillary Lymph Node Metastasis in Patients with Primary Breast Cancer. Biomed Res Int. 2022 Aug 10; 2022. https://doi.org/10.1155/2022/8616535
52. Lang DM, Peeken JC, Combs SE, Wilkens JJ, Bartzsch S. Deep learning based HPV status prediction for oropharyngeal cancer patients. Cancers. 2021 Feb 13; 13(4): 786. https://doi.org/10.3390/cancers13040786
53. Mi W, Li J, Guo Y, Ren X, Liang Z, Zhang T, Zou H. Deep learning-based multi-class classification of breast digital pathology images. Cancer Manag Res. 2021 Jun 10: 4605-17. https://www.tandfonline.com/doi/full/10.2147/CMAR.S312608
54. Hu W, Li C, Li X, Rahaman MM, Ma J, Zhang Y, et al. GasHisSDB: A new gastric histopathology image dataset for computer aided diagnosis of gastric cancer. Comput Biol Med. 2022 Mar 1; 142: 105207. https://doi.org/10.1016/j.compbiomed.2021.105207.
55. Zhao Y, Hu B, Wang Y, Yin X, Jiang Y, Zhu X. Identification of gastric cancer with convolutional neural networks: a systematic review. Multimedia Tools Appl. 2022 Mar; 81(8): 11717-36. https://doi.org/10.1007/s11042-022-12258-8
56. Tung CL, Chang HC, Yang BZ, Hou KJ, Tsai HH, Tsai CY, et al. Identifying pathological slices of gastric cancer via deep learning. J Formos Med Assoc. 2022 Dec 1; 121(12): 2457-64. https://doi.org/10.1016/j.jfma.2022.05.004
57. Gupta S, Kalaivani S, Rajasundaram A, Ameta GK, Oleiwi AK, Dugbakie BN. Prediction performance of deep learning for colon cancer survival prediction on SEER data. Biomed Res Int. 2022 Jun 16; 2022. https://doi.org/10.1155/2022/1467070
58. Rajinikanth V, Kadry S, Damaševičius R, Sankaran D, Mohammed MA, Chander S. Skin melanoma segmentation using VGG-UNet with Adam/SGD optimizer: a study. 3ed Int Conf Intell Comput Instrum Control Technol. 2022 Aug 11 (pp. 982-986). IEEE.https://doi.org/10.1109/ICICICT54557.2022.9917848 .
59. Tripathi M. Analysis of convolutional neural network based image classification techniques. J Innov Image Process. 2021 Jun; 3(02): 100-17. https://www.academia.edu/download/76640587/03.pdf .
60. Hany M. Chest ctscan images dataset, Kaggle, 2020. [Online]. https://www.kaggle.com/datasets/mohamedhanyyy/chest-ctscan-images. [Accessed 1 5 2022].
61. Mahdi GJ. A Modified Support Vector Machine Classifiers Using Stochastic Gradient Descent with Application to Leukemia Cancer Type Dataset. Baghdad Sci J. 2023; 17(4): 1255. https://bsj.uobaghdad.edu.iq/index.php/BSJ/article/view/4283
62. Hasan AM, Qasim AF, Jalab HA, Ibrahim RW. Breast Cancer MRI Classification Based on Fractional Entropy Image Enhancement and Deep Feature Extraction. Baghdad Sci J. 2023 Feb. 1; 20(1): 0221. https://bsj.uobaghdad.edu.iq/index.php/BSJ/article/view/6782

2024, 21(3): 1101-1118
https://dx.doi.org/10.21123/bsj.2023.8340
P-ISSN: 2078-8665 - E-ISSN: 2411-7986
Baghdad Science Journal

تقنيات التعلم العميق في المجال الطبي المتعلق بالسرطان: نموذج مجموعة نقل التعلم العميق للتنبؤ بسرطان الرئة.

عمر عبد اللطيف جاسم[1], محمد جواد عبد[1] و زينة هادي سعيد[2]

[1]قسم هندسة تقنيات الاجهزة الطبية, كلية الحكمة الجامعة, بغداد, العراق
[2] قسم تقنيات المختبرات الطبية, المعهد الطبي التقني-المنصور, الجامعة التقنية الوسطى, بغداد, العراق

الخلاصة

المشكلة: يعتبر السرطان أحد أكثر الأمراض فتكًا في العالم. يمكن أن يسهل التعلم الآلي وخوارزميات التعلم العميق طريقة التعامل مع السرطان لا سيما في مجال الوقاية من السرطان واكتشافه. إن للطرق التقليدية لتحليل بيانات السرطان محددات عديدة كما أنَّ بيانات السرطان تنمو بسرعة. هذا يجعل من الممكن للتعلم العميق المضي قدمًا بقدراته القوية على تحليل ومعالجة بيانات السرطان. الأهداف: تم في الدراسة الحالية تقديم نظام دعم طبي للتعلم العميق للتنبؤ بسرطان الرئة. الطرائق: تستخدم الدراسة ثلاثة نماذج مختلفة للتعلم العميق (EfficientNetB3 وResNet50 وResNet101) مع مفهوم نقل التعلم. تم تدريب النماذج الثلاثة باستخدام مجموعة بيانات لسرطان الرئة بالأشعة المقطعية المؤلفة من 1000 صورة وأربع فئات مختلفة للسرطان. تم تطبيق عملية Data Augmentation لحل مشكلة Overfitting وزيادة حجم البيانات وتعزيز عملية التدريب. تم أيضًا استخدام الدمج على مستوى الدرجة والتعلم التجميعي Ensemble Learning للحصول على أفضل أداء وحل مشكلة الدقة المنخفضة. تم تقييم جميع النماذج باستخدام معايير الدقة وPrecision وRecall وF1-score. النتائج: تظهر التجارب الأداء العالي لنموذج التعلم التجميعي بدقة 99.44٪، وهو أفضل من جميع المنهجيات الحديثة الحالية. الخلاصة: تظهر نتائج الدراسة الحالية الدقة العالية والمتانة للتعلم العميق لنقل المجموعة المقترحة باستخدام نماذج تعلم التحويل المختلفة.

الكلمات المفتاحية: التعلم التجميعي، التعلم العميق، الهندسة الطبية، تخمين السرطان، تعلم الآلة، سرطان الرئة، سرطان الصدر.